Appl. Phys. B 75, 899–902 (2002)
DOI: 10.1007/s00340-002-1051-0

Applied Physics B
Lasers and Optics

Rapid communication

D. MIKALAUSKAS
A. DUBIETIS✉
R. DANIELIUS

Observation of light filaments induced in air by visible picosecond laser pulses

Department of Quantum Electronics, Vilnius University, Saulėtekio Ave. 9, Bldg. 3, 2040 Vilnius, Lithuania

Received: 7 August 2002/Revised version: 12 September 2002
Published online: 11 December 2002 • **© Springer-Verlag 2002**

ABSTRACT We report the observation of light filaments produced by a picosecond laser pulse in the visible. The pulse trapped in the filamentary mode experiences large-scale self-phase modulation, with almost 100-fold spectral broadening along with apparent shortening of the leading edge. Spatial-temporal properties of the light filament reveal rather complex propagation dynamics.

PACS 42.65.Jx; 42.65.Tg

Optical guiding of an intense laser pulse in a plasma channel was demonstrated by Durfee and Milchberg almost a decade ago [1]. Some years later, Braun et al. reported self-guiding of an intense femtosecond pulse in air [2]. Since that time the effect of long-distance self-guided pulse propagation in air has attracted considerable attention [3–18]. There is now agreement that self-guiding of an intense laser pulse in gaseous media in general appears to be a result of dynamic balance between two competing non-linear effects: the Kerr effect, leading to self-focusing, and a defocusing effect of the electron plasma created through multiphoton ionization. In that way a single finite filament with the diameter of ~ 100 micrometers is formed. Even with a power well above the critical level for Kerr self-focusing, collapse of the beam is prevented, and the filament preserves its shape over tens of meters of propagation.

To date, filament formation has been extensively studied with picosecond and femtosecond pulses at ~ 800 and 248 nm, produced by Ti:sapphire driven laser systems. Recent findings revealed different spectral content of light filaments produced by different wavelengths: those excited by the IR pulses show generation of broad supercontinuum extending from UV to IR [6–8], whereas the UV-pulse-induced filaments exhibit much less spectral broadening [9, 10]. This is explained by large differences of peak intensity required for the filament formation. The critical intensity for the IR-induced filaments is as high as $\sim 4 \times 10^{13}$ W/cm^2 [11], since a large number of photons is required to initiate the ionization process (11 and 8 photons for nitrogen and oxygen molecules at 800 nm, respectively). The critical intensity for the UV filaments is considerably lower and ranges between $\sim 10^{11}$ and $\sim 10^{12}$ W/cm^2 [10, 12]. It requires only four and three photons to launch the ionization process for nitrogen and oxygen molecules, respectively. As was shown recently, photoionization of the oxygen molecules plays a key role in both cases [11]. However, powerful pulses in the visible are not easily accessible by the Ti:sapphire laser systems; therefore filament formation in this wavelength range is currently unexplored.

In this Letter we report the observations of light filaments produced by a 0.9-ps laser pulse at 527 nm (second harmonic of the Nd:glass laser). Measurements in spectral, spatial, temporal and combined spectral–spatial domains have been performed. The filaments in the visible are characterized by the broad self-phase-modulation (SPM) spectra and possess interesting spatial features not observed before. Temporal measurements point to apparent shortening of the pulse, which precedes the pulse splitting.

The experimental data were obtained using a CPA-based Nd:glass laser system TWINKLE, provided by Light Conversion Ltd., Lithuania. The laser system runs at a 10 Hz repetition rate and is capable of delivering a 0.9-ps pulse with an energy up to 5 mJ at the second-harmonic wavelength (527 nm). The focusing setup consists of two curved mirrors that allow the achievement of different effective focal lengths by varying the distance between them. The initial input beam FWHM diameter of 4.3 mm is resized to ~ 2 mm at the output of the focusing setup. Due to lack of space (the laboratory length is 16 m) the focusing setup was aligned to have an effective focal length of $f = 5$ m. To be precise, we have tested various focal lengths, starting with $f = 3.5$ m and ending with $f \approx 15$ m. However, with long focal distances the length of the light filament far exceeds the laboratory length, so being beyond our ability to perform measurements.

For filament characterization we split a fraction of the power by using a front reflection from a wedged fused-silica plate inserted at nearly grazing incidence. The light filament starts emerging at 1.6-mJ incident pulse energy. The length of the filament is a function of the

✉ Fax: +370-2/3660-06, E-mail: audrius.dubietis@ff.vu.lt

incident energy, yet it is not easy to estimate. While the starting point of the filament could be identified by the appearance of conical emission, the end point remains rather uncertain. Experimentally, with an incident energy of 4 mJ, spectral broadening is observed over ~ 10 m of propagation.

The amount of energy trapped within the filament was estimated to be in the order of ~ 0.9 mJ. This value was found to be fairly constant and not dependent on the incident energy in the range of 1.6–3.0 mJ. The energy was measured by transmitting the diffracting beam through the ~ 1.5 mm iris diaphragm, placed ~ 3 m away from the presumed filament end. The critical power for self-focusing of 527-nm pulses in air is $P_{\rm cr} = \lambda^2/2\pi n_0 n_2 \approx 1.4$ GW, taking the value of $n_2 = 3.2 \times 10^{-19}$ cm^2/W [8]. Assuming the FWHM diameter $d \approx 120\,\mu$m, we evaluated the intensity within the filament as $I_{\rm fil} \approx 6 \times 10^{12}$ W/cm^2. The obtained value is consistent with expectations and falls between those for IR and UV filaments.

The filament spectra were recorded by imaging the front face of the fused-silica plate onto the input slit of a multichannel spectrum analyzer OMA III (EG & G). Spectral broadening starts with the generation of blue-shifted components (Fig. 1a). The blue shift is likely a signature of the pulse interaction with plasma, as noted in [4, 13]. A characteristic peak and valley structure develops with the pulse propagation. With 3.4 mJ incident pulse energy we observed significant spectral broadening, which covers the entire visible spectral region. The shape of the filament spectrum, as measured 6 m away from the filament starting point, resembles that typically produced by strong SPM (see Fig. 1b). Blue-shifted spectral components have lower spectral intensity, and we attribute this effect in part to the inertial contribution to the non-linear refractive index of gas molecules [14, 15]. The envelope of the spectrum becomes more complex with propagation length. Blue-shifted spectral components drift out from the center of the filament, forming a new spatial structure. Red-shifted components indicate secondary chirping, as the temporal profile of the pulse undergoes dramatic changes. We also tested the spectral broadening with various effective focal lengths of the focusing setup ($f = 3.5$–10 m) and found that SPM-induced spectral broadening is present in all cases and possesses similar spectral features.

We observed some specific spatial properties of the light filament produced by the 527-nm pulse. First of all, the blue-shifted spectral components of the filament possess a larger angular spread than the red-shifted components (natural diffraction suggests the opposite). This could be explained in the following way. The initial pulse experiences strong chirping along with generation of a plasma channel. Naturally, the red-shifted spectral components appear in the leading edge of the pulse, where the plasma is not so dense, while the trailing edge of the pulse encounters a more dense region of the plasma and experiences a strong defocusing action, in agreement with the dynamic spatial replenishment model [5]. Moreover, spatial–spectral measurements suggest the presence of strong non-collinear four-wave mixing (see below) that leads to efficient off-axis generation of high-frequency spectral components, thus increasing the effective filament diameter in the blue spectral region. A combination of neutral and color filters allowed the recording of the filament spot at different wavelength regions (Fig. 2). Conical emission due to its considerably lower intensity is not visible. Images (a) and (b) show the filament spot after 6 m of propagation (the distance is measured from the beginning of the filament) in red (> 570 nm) and blue (< 490 nm) spectral regions, respectively. The FWHM diameters are 120 μm and 180 μm, for the red and the blue spectral components, respectively. Images (c) and (d) were recorded after 11 m of propagation. The spot size of the red components (c) is increased by a factor of 1.5, whereas two filaments with blue spectral content are clearly present. The FWHM diameter of each newly formed spot is as large as $\sim 800\,\mu$m.

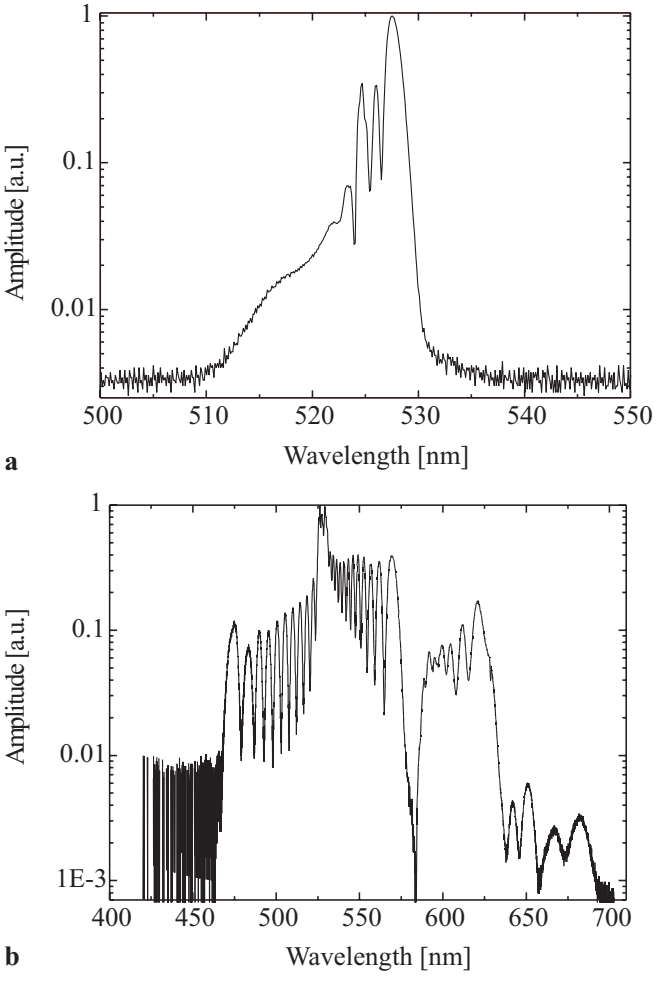

FIGURE 1 Filament spectra recorded at different incident energies: **a** 1.6 mJ, **b** 3.4 mJ

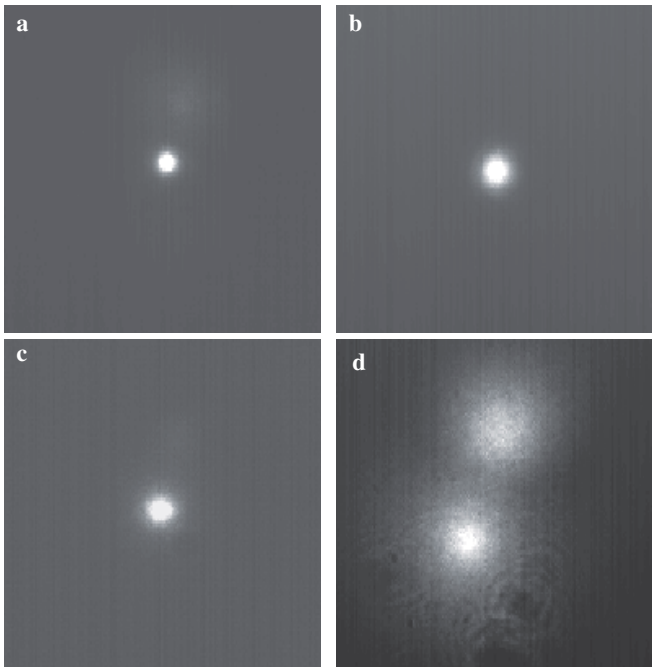

FIGURE 2 CCD camera images of the filament spots after 6 m (**a**, **b**) and 11 m (**c**, **d**) of propagation. Images on the *left* show yellow-red spectral components ($\lambda > 550$ nm), while images on the *right* show blue ($\lambda < 500$ nm) spectral components. The corresponding FWHM diameters for **a** and **b** are 120 and 180 micrometers, respectively

We note that this effect is associated with evolution of the pulse temporal envelope rather than with modulational instability. The latter effect is shown to have a strong influence in the initial filament formation stage [16], where the pulse temporal profile is still undistorted. The dynamic picture is much more complex, still being the main issue towards understanding the propagation of ultra-short pulses through the atmosphere.

Theoretical models predict pulse shortening and splitting [5, 8, 9, 17], with a final contest of soliton generation [18, 19]. Due to limited working space we could not perform temporal measurements along the filament as it propagates; nevertheless, we obtained some preliminary data in order to gather a qualitative impression of temporal features. Pulse-duration measurements were performed 16 m away from the focusing setup, where diffraction overtakes self-guiding; hence the intensity of the beam is reduced to a safe level. We employed a conventional scanning autocorrelator based on four-wave mixing in a 1-mm thick fused-silica plate. As expected, we observed apparent pulse shortening and reshaping versus incident energy. With an incident energy of 1.6 mJ (the filament length is several tens of centimeters) we measured a Gaussian pulse with a duration of 670 fs, i.e. somewhat shorter than the input one. With an increase of the input energy we observed noticeable pulse shortening – a 160-fs pulse was measured at 3.4-mJ input energy, as shown in Fig. 3. Third-order autocorrelation allowed the indication of the direction of the time axis, so that we found that the short pulse (at the leading edge) is associated with predominantly red-shifted spectral components. To this end, we observed additional red-shifted spectral broadening which, we believe, is invoked by a newly formed pulse.

Spectral–spatial features of the filament were recorded using a 600-l/mm diffraction grating. The low-resolution picture of the entire spectrum indicates the filament splitting: there exist two filaments with wavelengths less than 450 nm (Fig. 4). Figure 5 shows the angular distribution of the filament spectrum recorded after 11 m of propagation. Spectral components in the blue spectral region exhibit the development of an apparent off-axis structure, whereas a similar feature in the yellow-red side of the spectrum is far less prominent. The observed features are likely to be produced by the noncollinear four-wave mixing between the spectral components in the filament satisfying the geometrical phase-matching conditions, as suggested by Luther et al. [20]. The reason for the asymmetry of these features with respect to the pump wavelength remains unclear at the moment. However, this finding explains in part why the diameter of the blue-shifted spectral components is larger as compared to that of the red-shifted components.

In conclusion, we have observed light filaments produced by a green picosecond laser pulse in air. We estimate the filament intensity of $\sim 6 \times 10^{12}\,\mathrm{W/cm^2}$, thus being by an order of magnitude less than that for the IR filament formation. Filamentation in the visible is characterized by strong chirping, pointing to SPM as the

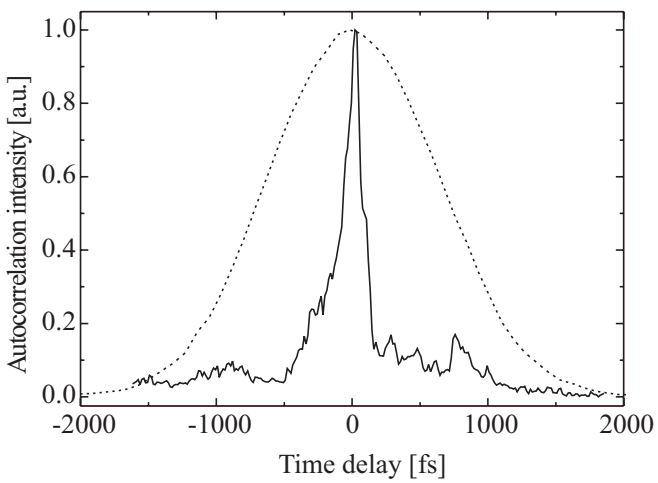

FIGURE 3 Autocorrelation traces: second-order autocorrelation trace of the input pulse (*dashed curve*), third-order autocorrelation trace of the filament produced by a 3.4-mJ incident pulse (*solid curve*)

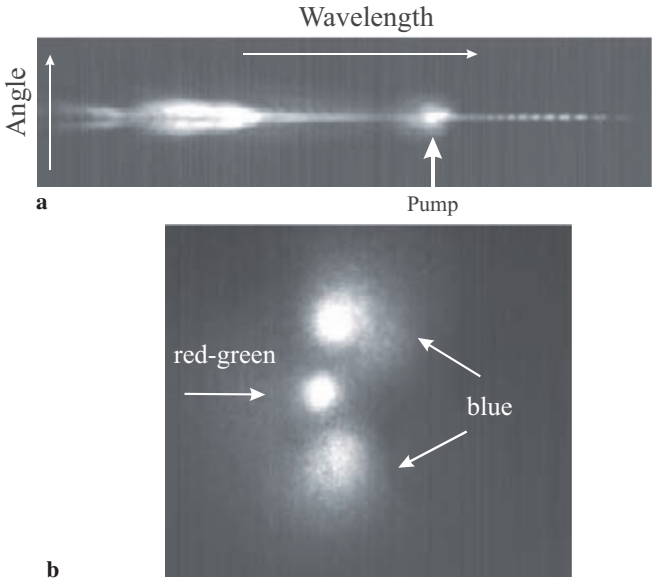

FIGURE 4 **a** Spectral–spatial image of the filament obtained using a 600-l/mm grating. Due to limited resolution only coarse features are visible. **b** RGB image of the filament. Intensities of spectral components in both images are arbitrary because of color filters

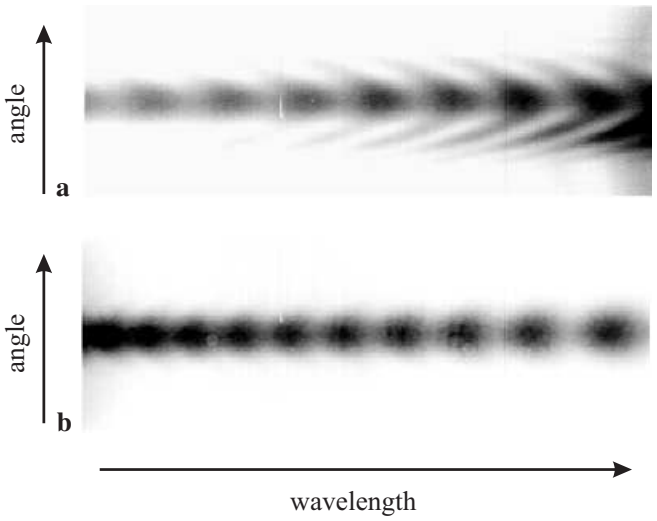

FIGURE 5 Angular distribution of spectral components in the filament, as measured after 11 m of propagation: **a** blue-shifted spectral components ($\lambda = 505$–520 nm), **b** red-shifted spectral components ($\lambda = 550$–580 nm)

main driving mechanism for the spectral broadening. The pulse temporal behavior shows apparent pulse shortening, in agreement with model predictions. We also notice that in the blue spectral region the filament splits in two; this effect can be explained by shortening and reshaping of the pulse. Moreover, clear signatures of four-wave mixing between the spectral components within the filament are observed, leading to the appearance of 'fish-bone' structures in the spatial–spectral domain.

ACKNOWLEDGEMENTS

The authors gratefully acknowledge discussions with Prof. A. Piskarskas and Dr. G. Valiulis, and thank I. Diomin for technical assistance.

REFERENCES

1 C.G. Durfee III, H.M. Milchberg: Phys. Rev. Lett. **71**, 2409 (1993)
2 A. Braun, G. Korn, X. Liu, D. Du, J. Squier, G. Mourou: Opt. Lett. **20**, 73 (1995)
3 E.T.J. Nibbering, P.F. Curley, G. Grillon, B.S. Prade, M.A. Franco, F. Salin, A. Mysyrowicz: Opt. Lett. **21**, 62 (1996)
4 O.G. Kosareva, V.P. Kandidov, A. Brodeur, C.Y. Chien, S.L. Chin: Opt. Lett. **22**, 1332 (1997)
5 M. Mlejnek, E.M. Wright, J.V. Moloney: Opt. Lett. **23**, 382 (1998)
6 J. Kasparian, R. Sauerbrey, D. Mondelain, S. Niedermeier, J. Yu, J.-P. Wolf, Y.-B. Andre, M. Franco, B. Prade, S. Tzortzakis, A. Mysysrowicz, M. Rodriguez, H. Wille, L. Wöste: Opt. Lett. **25**, 1397 (2000)
7 P. Rairoux, H. Schillinger, S. Niedermeier, M. Rodriguez, F. Ronnenberger, R. Sauerbrey, B. Stein, D. Waite, C. Wedekind, H. Wille, L. Wöste, C. Ziener: Appl. Phys. B **71**, 573 (2000)
8 A. Couairon, S. Tzortzakis, L. Berge, M. Franco, B. Prade, A. Mysyrowicz: J. Opt. Soc. Am. B **19**, 1117 (2002)
9 S. Tzortzakis, B. Lamouroux, A. Chiron, S.D. Moustaizis, D. Anglos, M. Franco, B. Prade, A. Mysyrowicz: Opt. Commun. **197**, 131 (2001)
10 S. Tzortzakis, B. Lamouroux, A. Chiron, M. Franco, B. Prade, A. Mysyrowicz, S.D. Moustaizis: Opt. Lett. **25**, 1270 (2000)
11 J. Kasparian, R. Sauerbrey, S.L. Chin: Appl. Phys. B **71**, 877 (2000)
12 J. Schwarz, P. Rambo, J.-C. Diels, M. Kolesik, E.M. Wright, J.V. Moloney: Opt. Commun. **180**, 383 (2000)
13 T. Lehner, N. Auby: Phys. Rev. E **61**, 1996 (2000)
14 E.T.J. Nibbering, G. Grillon, M.A. Franco, B.S. Prade, A. Mysyrowicz: J. Opt. Soc. Am. B **14**, 650 (1997)
15 J.-F. Ripoche, G. Grillon, B. Prade, M. Franco, E. Nibbering, R. Lange, A. Mysysrowicz: Opt. Commun. **135**, 310 (1997)
16 S. Tzortzakis, L. Berge, A. Couairon, M. Franco, B. Prade, A. Mysyrowicz: Phys. Rev. Lett. **86**, 5470 (2001)
17 A. Chiron, B. Lamouroux, R. Lange, J.-F. Ripoche, M. Franco, B. Prade, G. Bonnaud, G. Riazuelo, A. Mysyrowicz: Eur. Phys. J. D **6**, 383 (1999)
18 I.G. Koprinkov, A. Suda, P. Wang, K. Midorikawa: Phys. Rev. Lett. **84**, 3847 (2000)
19 L. Berge, A. Couairon: Phys. Rev. Lett. **86**, 1003 (2001)
20 G.G. Luther, A.C. Newell, J.V. Moloney, E.M. Wright: Opt. Lett. **19**, 789 (1994)